Combined finite-discrete element analysis of rock slope stability under dynamic loading

Andrea Lisjak & Giovanni Grasselli
Geomechanics Research Group, Lassonde Institute, Department of Civil Engineering – University of Toronto, Toronto, Ontario, Canada

ABSTRACT
Rock slope instability phenomena have been often correlated to seismic activity. Therefore, earthquake-induced ground motion should be taken into account when performing slope stability analysis in seismically active areas of the world. In the present study, the combined finite-discrete element (FEM/DEM) numerical method is proposed as a tool to assess stability of rock slopes subjected to seismic shaking. Main advantages of FEM/DEM include the capability of simulating interaction between multiple blocks, rock breakage and fragmentation and evaluating failed block trajectory and run-out distance. Algorithmic developments such as absorbing boundary conditions and rock joint shear strength degradation model were specifically introduced to correctly model stress wave propagation and joint behaviour. Effectiveness of the method was proved by means of two conceptual models relative to a planar failure and a rock fall, respectively.

RÉSUMÉ
Phénomènes d'instabilité des pentes ont été souvent déclenché par l'activité sismique. Par conséquent, dans l'analyse de stabilité des pentes localisées dans des zones sismiquement actives, il faut considérer les effets induits par le tremblement de terre. Dans cette étude, la méthode numérique à élément finis / élément discrets (FEM / DEM) est utilisé pour évaluer la stabilité des pentes rocheuses soumis à des vibration sismiques. Principaux avantages du FEM / DEM sont la capacité de simuler (i) l'interaction entre plusieurs blocs, (ii) la fragmentation des blocs en roche, et (iii) la trajectoire et la distance de l'écoulement rocheuse. Dans ce papier, des spécifiques algorithmes de dissipation d'énergie a l'impact et de dégradation de la résistance de cisaillement des joints en roche on été utilisé. Deux exemples de instabilité de pente sont présentés pour démontrer l'utilisation de la méthode.

1 INTRODUCTION

Several rock slope instability cases around the world have been correlated to seismic activity (e.g., Wilson et al. 1984, Kobayashi et al. 1990) over the past few decades. Therefore, earthquake-induced ground motion should be taken into account when performing slope stability analysis in seismically active areas of the world (Wyllie and Mah 2004).

When slope stability analysis under dynamic loading has to be performed, a seismic hazard analysis is first carried out to characterize the ground motion at the site under investigation and provides the input parameters for the stability analysis (Abrahamson 2000). These generally consist in either the peak ground acceleration (PGA) or the ground acceleration-time history.

For the simple case of a rock block sliding on a planar surface, two different design procedures have been traditionally used to incorporate the effect of ground motion in the stability analysis: the pseudo-static method and the Newmark's analysis. In the pseudo-static method an horizontal force, taken as a fraction of the PGA, is added to the slope in a direction out of the face. This method, although generally conservative, is highly inaccurate because does not account for stress wave transient effects, sensitivity of the slope to seismic deformation and decrease in shear strength with tangential displacement. A more accurate method was proposed by Newmark (1965). With this procedure acceleration history at the block base is integrated in time to determine its final displacement, which is then compared to a maximum allowed value based on rock joint conditions. Being both procedures analytical, simplified block and joint geometries are assumed and no information can be obtained regarding the post-failure movement of a failed block.

More recently, the application of numerical methods has been investigated aimed at providing simulation tools able to dynamically simulate earthquake-induced rock slope instability phenomena including initial failure mechanisms and post-failure dynamics. More specifically, the Discontinuous Deformation Analysis (DDA) method (Shi and Goodman 1995) was employed among others by Sasaki et al. (2004) and Haztor et al. (2004), while UDEC (Itasca Consulting Group) was used, for example, by Bhasin and Kaynia (2004).

In the present study the combined finite-discrete element method (FEM/DEM) is proposed as an alternative to assess stability of rock slopes subjected to seismic shaking in the cases of planar failure and rock fall. Main advantages of FEM/DEM include the possibility of simulating interaction between multiple blocks, rock breakage and fragmentation and evaluating failed block trajectory and run-out distance. The FEM/DEM code used in this study is based on the original Y-code of Munjiza (2004). The code has been the subject of ongoing research and development by the Geomechanics Group at the University of Toronto.

2 THE COMBINED FINITE-DISCRETE ELEMENT METHOD

The combined finite-discrete element method is a numerical tool pioneered by Munjiza et al. (1995) for the dynamic simulation of multiple deformable and fracturable bodies. Within the framework of FEM/DEM, discrete element method (DEM) principles are used to model interaction between different solids, whose deformation is analyzed by finite element analysis (FEM). A unique feature of such a numerical tool is its capacity to model the transition from continuous to discontinuous behaviour by explicitly considering fracture and fragmentation processes. Since an explicit time-marching scheme is used to integrate Newton's equations of motion, fully dynamic simulations can be performed.

Three of the key-algorithms of the method (i.e., the fracture model, the contact interaction algorithm and the dissipative impact model) are discussed in the following.

2.1 Fracture model

A combined single and smeared crack model (Munjiza et al., 1999), also known as the discrete crack model, is implemented in the FEM/DEM code used for this study. Rock behaves elastically until the strength limit, defined by a Mohr-Coulomb criterion with tension cut-off, is reached. Upon overcoming the elastic limit, a new fracture is driven across the interface between adjacent triangular finite elements. Material separation processes and crack process zone are modelled by means of cohesive elements as a gradual strength reduction governed by a softening law. Material strength mobilization is represented by a shear and normal bonding stresses, τ and σ, which are generated by the separation of the crack edges. As depicted in Figure 1 and 2, these stresses are assumed to be a function of crack opening, o, and sliding distance, s. Fracture behaviour is ultimately controlled by the following input parameters: tensile strength f_t, elastic modulus E, shear strength f_s, derived from cohesion c and internal friction angle ϕ, and fracture energy release rate G_f.
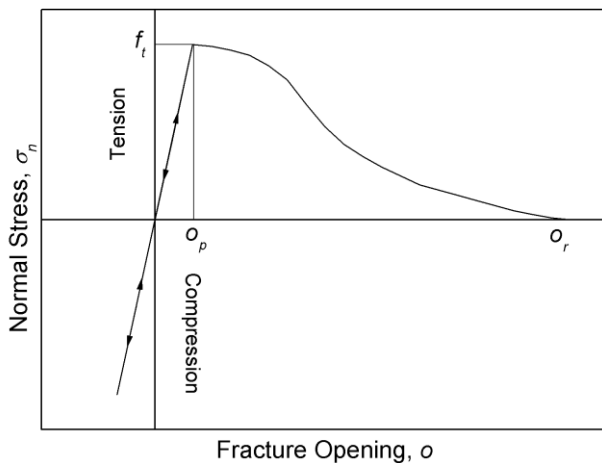

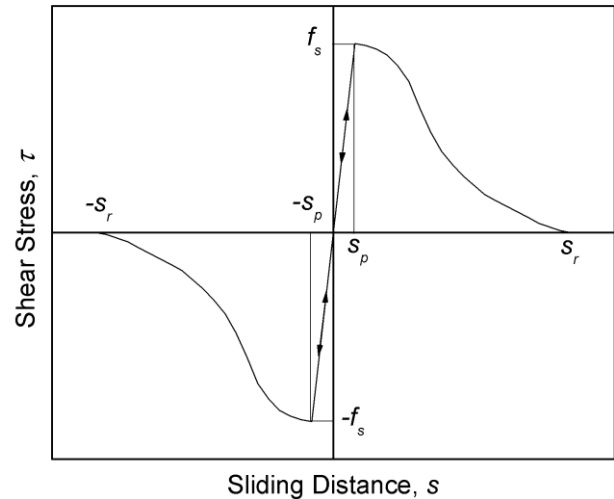Figure 1. Fracture model constitutive law relating normal stress to fracture opening.

Figure 2. Fracture model constitutive law relating shear stress to fracture sliding distance.

Although re-meshing is not performed ahead of the crack tip, by using sufficiently fine meshes the direction of fracture propagation can be correctly captured.

2.2 Interaction between discrete elements

Contact interaction has a fundamental importance in FEM/DEM since it influences the behaviour of systems formed by many interacting distinct elements. As soon as two discrete bodies are detected in contact, the interaction algorithm is applied to calculate forces between discrete bodies. A penalty function method (Munjiza and Andrews, 2000) is used for the interaction algorithm. In normal direction contacting couples tend to penetrate into each other, generating distributed contact forces, which depend on the shape and size of the overlap between the two bodies. Body impenetrability condition is reached as a limit condition for normal penalty values that tend to infinity. In tangential direction, a Coulomb-type friction law is used to calculate shear interaction forces and simulate rock joint frictional behaviour (Mahabadi et al., 2010).

2.3 Dissipative impact model

In the field of rock fall numerical modelling, correctly simulating the experimentally observed reduction in boulder velocity upon impact is crucial for predicting the trajectory of falling blocks. Since most of the energy dissipation occurs at the contact between colliding bodies (Dorren, 2003), the impact model plays a key role in the numerical simulation of the phenomenon. The contact interaction algorithm illustrated in Section 2.2 computes contact stresses based on the principle of energy conservation and it is therefore unable to capture inelastic processes such as rock crushing and slope plastic deformation that occur during rock impacts. A dissipative contact model (Lisjak and Grasselli, 2010) is therefore available in FEM/DEM aimed at overcoming this major limitation.

In this model, the constitutive law relating contact stress, σ_c, to the contact normalized overlapping area, a, as defined by Munjiza and Andrews (2000), is varied between the loading and unloading phase of the impact:

$$\sigma_c = \begin{cases} p \cdot a & \text{(loading curve)} \\ A \cdot a^B & \text{(unloading curve)} \end{cases} \quad [1]$$

where p is the compressive stiffness of the boulder-slope interface; A is coefficient automatically determined by the algorithm so that the relationship goes back to the origin; and B is the parameter that controls the amount of energy dissipated. During loading the contact stress increases linearly as the penetration increases, while during unloading phase of the contact kinetic energy is removed from the colliding block by decreasing the contact stiffness based on a power law. As can be observed in Figure 3, only a fraction of the total potential energy stored is returned to the block as kinetic energy, resulting in a decrease of block velocity.
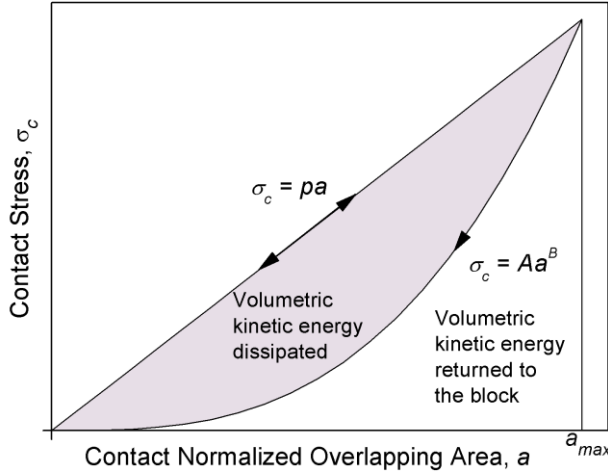

Figure 3. Elastic-power damping contact constitutive law used to simulate the effect on the block of the soil inelastic behaviour during impacts. Volumetric kinetic energy is defined as kinetic energy divided by block volume.

3 SEISMIC ANALYSIS WITH FEM/DEM

Introducing a seismic load in a FEM/DEM slope model requires special treatment of far-field boundaries, seismic source and model material properties. Details relative to this procedure are discussed in the following together with the implementation of a new rock joint shear strength degradation model, introduced to capture the joint shear strength reduction caused by earthquake-induced ground movements.

3.1 Absorbing boundaries

Since the combined finite-discrete element method requires finite computational domains but slope stability analysis involves a semi-infinite medium (i.e., the ground), the need for artificial far-field boundary conditions naturally arises. When performing pseudo-static stress-strain analysis, pins or rollers are generally chosen to constrain boundary nodes of the model. However, in dynamic problems, these boundary conditions may cause unrealistic reflections of outward propagating stress waves. Although the simplest solution to this problem would be to extend the domain boundaries far enough so that the region of interest would not be influenced by boundary effects, due to the high speed of elastic waves in rocks, this solution is computationally impractical. A valid alternative is represented by absorbing (or non-reflecting) boundary conditions. This special type of boundaries allows the necessary energy radiation, which is needed to perform dynamic stress analysis in unbounded media. Among the different absorbing boundary conditions available in the literature (Givoli, 1991), the local solution proposed by Lysmer and Kuhlemeyer (1969) was implemented because of its natural suitability for the explicit mechanical solver of FEM/DEM. With this approach, viscous boundary tractions are used to numerically absorb kinetic energy of incident waves. For a wave approaching a vertical boundary segment with particle velocity (v_x, v_y) these tractions are equal to:

$$\begin{cases} f_x = -\rho c_p \frac{\partial v_x}{\partial t} \\ f_y = -\rho c_s \frac{\partial v_y}{\partial t} \end{cases} \quad [2]$$

where c_p and c_s are the material p- and s-wave speed, respectively, which depend on the Lame's constants, μ and l, and density, ρ, through:

$$\begin{cases} c_p = \frac{l+2\mu}{\rho} \\ c_s = \frac{2\mu}{\rho} \end{cases} \quad [3]$$

3.2 Seismic source and stress wave propagation

Seismic shaking is inputted in a FEM/DEM slope model by specifying either the acceleration-time or velocity-time history in x- and y-direction of a finite element node internal to the model domain. This approach is based on the method originally proposed and implemented in a DDA code by Sasaki et al. (2004). By doing so, recorded seismograms can be directly applied to the numerical model without any assumptions regarding, for instance, the stress wave frequency spectrum.

In order to avoid unrealistic seismic wave reflections, the aforementioned absorbing boundaries are introduced at the bottom and lateral sides of the model. Since this type of boundary condition does not place any kinematic constraint on the model, specific devices are used to avoid downward movement of the model. In particular, body forces (i.e., gravity) are set to zero within the slope base region of the model and its inertia artificially

increased, such that movement under the effects of interaction with gravity-loaded upper blocks are negligible. From a numerical point of view, inertia increase is obtained by using a high density value together with a proportional increase in model stiffness, so that the correct elastic wave speed is still captured. Boundary conditions and loads are graphically summarized in the schematics of Figure 4.
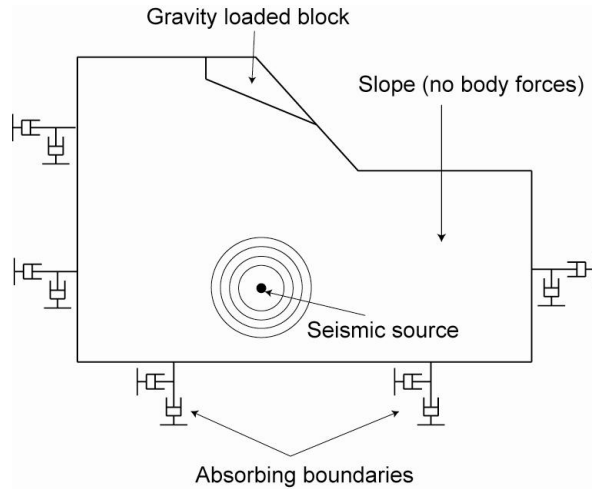

Figure 4. Loads and boundary conditions adopted in FEM/DEM to model rock slopes under seismic loading.

3.3   Rock joint shear strength degradation

The actual shear behaviour of discontinuity surfaces in rock slopes depends upon several factors including the surface roughness, the applied normal stress and the amount of shear displacement (Wyllie and Mah, 2004).
    When numerically modelling rock joint behaviour under dynamic loading, correctly capturing the variation of shear strength as a function of shear displacement is of the utmost importance. Experimental evidence indicates that during rock joint shearing, surface asperities are progressively damaged resulting in lower roughness value and consequently reduced frictional resistance. Under seismic loading, the induced amount of shear displacement may be such that the residual shear strength is reached causing the failure of the slope. Thus, following the approach adopted by Mahabadi and Grasselli (2010), a rock joint shear strength degradation model was implemented in FEM/DEM. As depicted in Figure 5, the shear stress, τ, initially increases linearly as a function of the shear displacement, u, with slope given by a tangential penalty parameter, p_t. Upon reaching the peak shear strength value, τ_p, the shear strength remains constant until the displacement overcomes a peak displacement value, u_p. If the joint continues to slide a hyperbolic decay-function is applied to degrade the shear strength as a function of displacement:

$$\tau(u) = \tau_r + \left(\tau_p - \tau_r\right)u_p/u \qquad [4]$$

where τ_r is the residual shear strength. Peak and residual shear strengths are defined by a Coulomb friction law:

$$\begin{cases} \tau_p = \sigma_n \tan \varphi_p \\ \tau_r = \sigma_n \tan \varphi_r \end{cases} \qquad [5]$$

where σ_n is the normal stress acting on the surface, and φ_p and φ_r are the peak and residual friction angles, respectively.
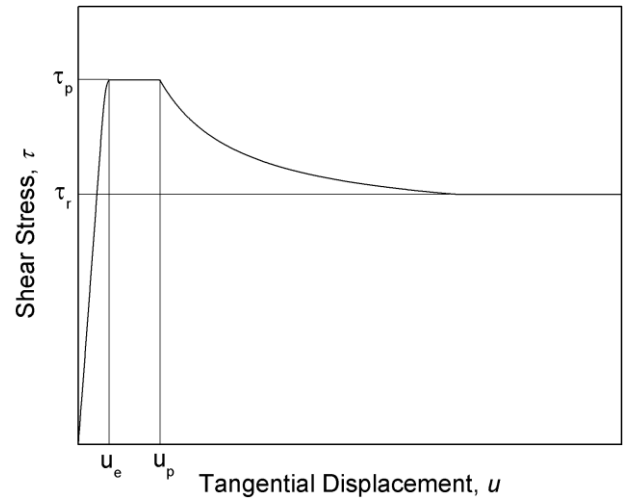

Figure 5. Rock joint shear stress as a function of tangential displacement.

4   NUMERICAL EXAMPLES

Two idealized examples of rock slope instability were chosen to better illustrate the application of FEM/DEM to modelling failure under dynamic loading.

4.1   Planar slide

The conceptual model depicted in Figure 6 was set up in order to show the potential effect of an earthquake on the stability of a block sliding over a planar discontinuity. It consists of a 30 m high rock cut with a face angle of 45° and a continuous discontinuity dipping at 25° out of the slope face and forming a sliding block.
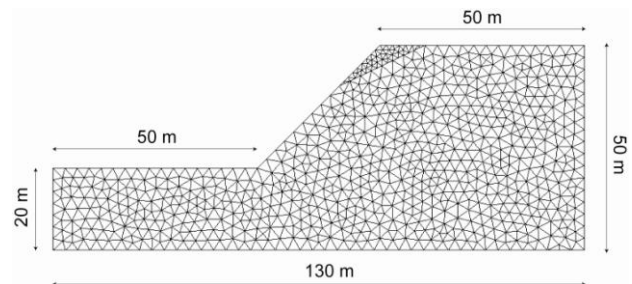

Figure 6. Planar failure model geometry and mesh.

The slope was modelled as an infinitely elastic medium while the sliding block was allowed to break. Shear strength degradation model illustrated in Section 3.3 was adopted to characterize the shear performance of the planar discontinuity. Material properties reported in Table 1 were assigned to the model.

Table 1. Material properties for the planar failure model

	Slope	Block	Joint
Young's modulus (GPa)	1	1	n/a
Poisson's ratio (-)	0.25	0.25	n/a
Peak friction angle (^{o})	n/a	45	40
Residual friction angle (^{o})	n/a	n/a	20
Cohesion (MPa)	n/a	10	0
Tensile strength (MPa)	n/a	5	0
Specific fracture energy (J/m^2)	n/a	1	n/a
Peak displacement (mm)	n/a	n/a	50

A preliminary analysis under static loading conditions was first carried out to verify the numerical results against the limit equilibrium method (LEM) solution. A critical peak joint friction angle of 25.6^o was numerical calculated versus a LEM critical value of 25°.

To correctly simulate the slope behaviour under dynamic loading the approach explained in Section 3.2 was applied for what concerns model boundary conditions and seismic input type. A sinusoidal shear wave with frequency, *f*, equal to 2 Hz was propagated inside the model for a duration, T, of 10 s by imposing a velocity-time history at the source node:

$$v(t) = v_{max} sin(2\pi f t) \qquad [6]$$

where the maximum ground velocity, v_{max} = 0.159 m/s, was derived from a value of the peak ground acceleration equal to 2 m/s^2 = 0.2g as follows:

$$v_{max} = a_{max}/(2\pi f) \qquad [7]$$

Joint peak friction angle was increased to 40° (i.e., stable value condition under static loading) with a residual value of 20°. The influence of a weak infilling was simulated by assigning a peak displacement value equal to 5 cm.

As can be observed in the simulation sequence illustrated in Figure 7, the slippage accumulation at the base of the block due to the cyclic dynamic load is sufficient to reduce the joint strength to the residual value causing the catastrophic failure of the rock block.
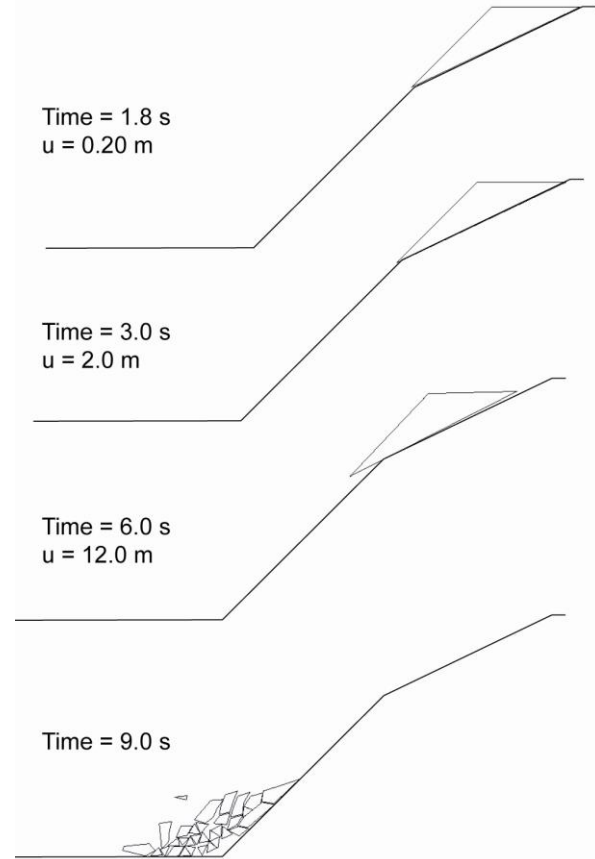

Figure 7. Planar failure simulation sequence indicating the joint shear displacement, *u.*

In order to prove the importance of the role played by the shear strength degradation, the same simulation was re-ran with residual friction angle equal to peak friction angle. A total displacement of 80 cm was induced by the earthquake, however the new slope configuration went back to stable conditions after ceasing the seismic shaking. In other words, for the case under analysis neither the variation of geometrical configuration nor the inertial effects induced by the earthquake were sufficient to cause the failure of the block if the shear strength was not reduced to a lower residual value.

4.2 Rock fall

An example of earthquake-induced rock fall was simulated in its entirety and complexity from the triggering process to its dynamic evolution. Design parameters such as rock fall kinetic energy, run-out distance and final fragmentation and material distribution were extracted from the simulation.

The slope geometry of the planar failure model was used while the single sliding block substituted by several rock boulders (Figure 8). Also, a 4 m high rigid interceptive wall was placed at 35 m from the toe of the slope.
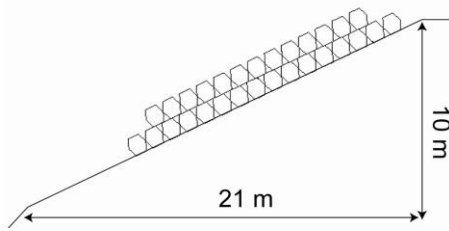
Figure 8. Top part of the slope with loosened rock boulders.

An actual seismogram recorded during the El Centro Earthquake in the Imperial Valley (California, USA) was directly imported as numerical seismic source (Pacific Earthquake Engineering Research Center). In particular, the North-South and Up-Down accelerograms shown in Figure 9 and 10 were integrated in time and inputted as horizontal and vertical velocity-time histories, respectively.
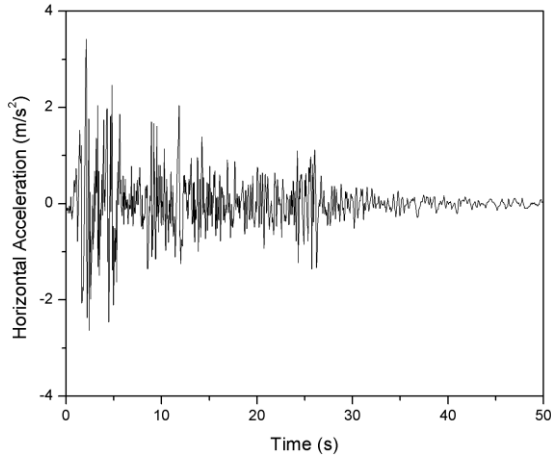

Figure 9. El Centro Earthquake North-South accelerogram (from Pacific Earthquake Engineering Research Center).
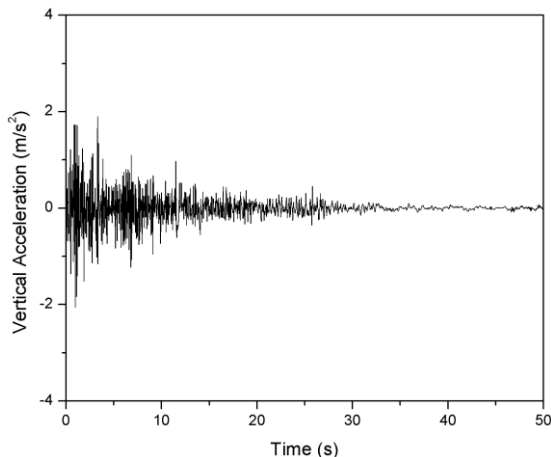

Figure 10. El Centro Earthquake Up-Down accelerogram (from Pacific Earthquake Engineering Research Center).

As can be observed in Figure 11, ground oscillatory motion impressed by the earthquake causes the instability of all 29 blocks which start rolling and sliding downhill. Notice that a preliminary static analysis had instead revealed unstable conditions only for the first 15 blocks.

In this case, instability does not arise only from the reduction of the frictional strength to residual values, as occurred in the sliding model, but also from the induced inertial forces which cause the rotation of single blocks triggering an overall rolling mode of motion of the fall.
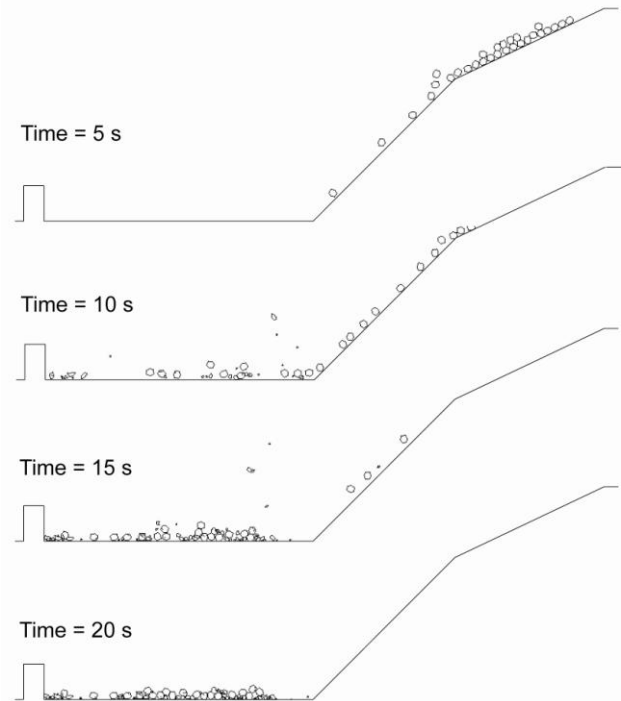

Figure 11. Rockfall simulation sequence.

In the second part of the simulation, the trajectories of falling blocks were reproduced together with the final material distribution at the toe of the slope. Evolution of rockfall total kinetic energy, a fundamental protective measure design parameter, as a function of time is reported in the graph of Figure 12.

5   SUMMARY AND CONCLUSIONS

In the present study, a new modelling approach, based on the combined finite-discrete element method (FEM/DEM), has been proposed to simulate the behaviour of rock slopes subjected to seismic loading. Absorbing boundary conditions were developed to correctly model stress wave propagation in unbounded media while a rock joint shear strength degradation model was introduced to simulate the shear strength reduction as a function of earthquake-induced joint tangential displacement. Effectiveness of the approach was demonstrated by means of two conceptual
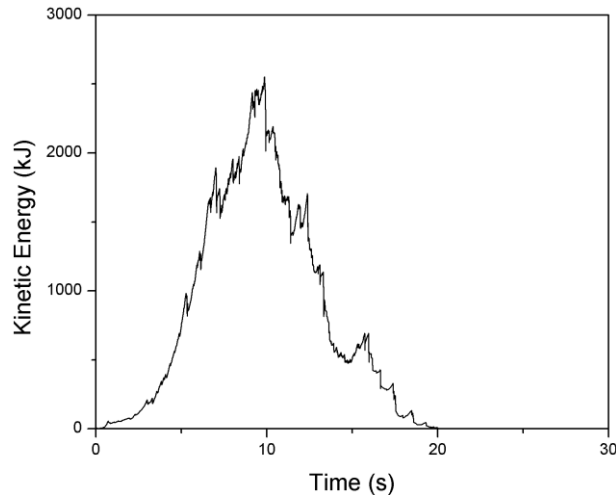
Figure 12. Evolution of rockfall total kinetic energy with time.

models, relative to a planar failure and a multiple rock block fall, respectively.

Main limitation of the current study is represented by the assumptions relative to the slope failure mechanism. Since the base of the slope is modelled as an elastic medium, only sliding along pre-existing discontinuities or rigid-body instability due to seismic induced inertial effects are possible failure modes in the FEM/DEM analyses carried out. Therefore, future work will focus on simulating fully fracturable rock masses whereby failure due to a combination of intact material breakage and sliding/opening along rock joints is allowed. This future development, together with the introduction of a Discrete Fracture Network and a hydro-mechanical coupling, will expand the field of application of FEM/DEM to a broader range of problems including open pits and gravity dams. Finally, the algorithms will be extended to a three dimensional version of the code currently under development.

ACKNOWLEDGEMENTS

REFERENCES

Abrahamson, N.A. 2000. State of the practice of seismic hazard evaluation, *GeoEng*2000, Melbourne, Australia.

Bhasin, R. and Kaynia, A.M. 2004. Static and dynamic simulation of a 700-m high rock slope in western Norway, *Engineering Geology,* 71: 213-226.

Dorren, L.K.A. 2003. A review of rockfall mechanics and modelling approaches, *Progress in Physical Geography,* 27: 69-87.

Givoli D. 1991. Non-reflecting boundary conditions, *Journal of Computational Physics,* 94: 1-29.

Hatzor, Y., Arzi, A., Zaslavsky, Y. and Shapira, A. 2004. Dynamic stability analysis of jointed rock slopes using the DDA method: King Herod's Palace, Masada, Israel *International Journal of Rock Mechanics and Mining Sciences,* 41(5): 813-832.

Kobayashi, Y., Harp, E.L. and Kagawa, T. 1990. Simulation of rockfalls triggered by earthquakes, *Rock Mechanics and Rock Engineering,* 23: 1-20.

Lisjak, A. and Grasselli, G. 2010. Rock impact modelling using FEM/DEM, *5th International Conference on Discrete Element Methods,* London, UK.

Lysmer, J. and Kuhlemeyer, R. 1969. Finite dynamic model for infinite media, *Journal of the Engineering Mechanics Division,* ASCE, 95(EM4): 859-876.

Mahabadi, O.K., Grasselli, G., and Munjiza, A. 2010. Y-GUI: A graphical user interface and pre-processor for the combined finite-discrete element code, Y2D, incorporating material heterogeneity, Computers & Geosciences, 36(2): 241-252.

Mahabadi, O.K. and Grasselli, G. 2010. Implementation of a rock joint shear strength criterion inside a combined finite-discrete element method (FEM/DEM) code, *5th International Conference on Discrete Element Methods,* London, UK.

Mahabadi, O.K., Lisjak, A., Grasselli, G., Lukas T. and Munjiza, A. 2010. Numerical modelling of a triaxial test of homogeneous rocks using the combined finite-discrete element method, *European Rock Mechanics Symposium (Eurock) 2010,* Balkema, Lausanne, Switzerland, 173-176.

Munjiza, A., 2004. The Combined Finite-Discrete Element Method, John Wiley & Sons, Hoboken, NJ, USA.

Munjiza, A. and Andrews K. 2000. Penalty function method for combined finite-discrete element systems comprising large number of separate bodies, *International Journal for Numerical Methods in Engineering,* 49(11): 1377-1396.

Munjiza, A., Andrews, K. and White, J. 1999. Combined single and smeared crack model in combined finite-discrete element analysis, *International Journal for Numerical Methods in Engineering,* 44(1111): 41-57.

Munjiza, A., Owen, D.R.J. and Bicanic, N., 1995. A combined finite-discrete element method in transient dynamics of fracturing solids, *Engineering Computations,* 12: 145-174.

Newmark, N.M. 1965. Effects of earthquakes on dams and embankments, *Geotechnique,* 15: 139-160.

Sasaki, T., Hagiwara, I., Sasaki, K., Yoshinaka, R., Ohnishi, T. and Nishiyama, R. 2004. Earthquake response analysis of rockfall models by discontinuous deformation analysis, *American Rock Mechanics Symposium 2004,* ARMA, Houston, USA.

Shi, G.-H. and Goodman, R.E. 1985. Two dimensional discontinuous deformation analysis, *International Journal for Numerical and Analytical Methods in Geomechanics,* 9: 541-556.

Wilson, R.C., Wieczorek, G.F., Keefer, D.K., Harp, E. and Tannaci, N.E. 1985. Map showing ground failures from the Greenville/Mount Diablo earthquake sequence of January 1980, Northern California, U.S.G.S. Map MF-1711.

Wyllie, D.C. and Mah, C.W. 2004. *Rock Slope Engineering: civil and mining*, 4th ed., Spon Press, New York, NY, USA.